Journal of Alloys and Compounds 505 (2010) 824–831

Contents lists available at ScienceDirect

Journal of Alloys and Compounds

journal homepage: www.elsevier.com/locate/jallcom

High temperature tribological properties of NiCrBSiCFe plasma-sprayed coating on austenitic stainless steel substrate

N.L. Parthasarathi, Muthukannan Duraiselvam*

Department of Production Engineering, National Institute of Technology, Tiruchirappalli 620015 Tamil Nadu, India

ARTICLE INFO

Article history:
Received 9 March 2010
Received in revised form 17 June 2010
Accepted 24 June 2010
Available online 23 July 2010

Keywords:
NiCrBSiCFe
Plasma spraying
Mechanical properties
Wear
Abrasion

ABSTRACT

In this study, the microstructural features, mechanical properties and dry sliding wear characteristics of NiCrBSiCFe plasma-sprayed on AISI 316 austenitic stainless steel (ASS) substrate were investigated. The coatings obtained were defect-free and metallurgically bonded to the substrate. Wear tests were carried out at 1 m/s sliding velocity under the load of 20 N for 2000 m sliding distance at various atmospheric conditions like room temperature, 150, 250 and 350 °C using a EN-8 medium carbon steel pin as a counterface material. The properties namely coating density, microhardness, coefficient of friction (CoF), wear resistance of the plasma-sprayed coating were studied. NiCrBSiCFe plasma-spray coated steel substrate showed superior wear resistance properties than the uncoated steel substrate in all the temperatures. The average wear resistance values of uncoated and NiCrBSiCFe coated material are 129 and 540 m/mm^3, respectively. Thereby, the sliding wear resistance was improved up to four times more than that of the uncoated material. In wear test carried out at 350 °C, the coated substrates showed relatively lesser wear than in other temperatures due to the iron and chromium oxide formation, which acted as a protective layer. This was evident from X-ray diffraction studies (XRD). In addition, the shallow ploughing mode of wear reduced the severity of material removal at 350 °C. Using scanning electron microscope (SEM) pictures, the wear properties of the coated steel substrate were evaluated in terms of plastic deformation, material transfer and abrasion.

1. Introduction

Austenitic stainless steels are extensively employed in high temperature parts of advanced gas-cooled reactor as constructional materials. Even though surfaces in sliding contact are designed where possible to avoid stainless-on-stainless contacts, these combinations inevitably occur in many components, e.g. boilers, metallic insulation packs and fuel assemblies. The friction and reciprocating unlubricated wear of type AISI 316 ASS on itself was investigated in air at room temperature in the load range 8–50 N. A model of the wear process was developed in terms of the interaction of asperities to form adhesive transfer platelets which agglomerate to layered prows [1]. The wear of an AISI 316 ASS has been studied in a variety of gaseous atmospheres at constant load and sliding speed under reciprocating conditions. The environments reported include air, CO_2, argon and partial vacuum. The wear debris in all cases was essentially metallic and its rate of production per unit length was constant with sliding distance [2]. The influence of melt texturing on the structural and superconductive properties of plasma-sprayed $Bi_2Sr_2CaCu_2O_3$ and $YBa_2Cu_3O_3$ layers on stainless steel and nickel substrates with a Yttria stabilized zirconia buffer layer was studied by Hemmes et al. [3]. Room temperature tests on air and vacuum plasma-sprayed TiC–NiCrBSi coatings using a pin-on-disk tribometer at various loads and sliding speed have been performed in order to understand the effects of the parameters on the coating wear and friction behaviour. Results have shown that load, sliding speed and the plasma-spray process affect the wear resistance and the friction behaviour of thermally sprayed coatings. Higher loads during sliding led to higher wear rates for both air and vacuum plasma-sprayed coatings [4]. The dry sliding behaviour of an austenitic stainless steel (ASS) and a duplex 2205 austenitic-ferritic stainless steel was investigated. The evolution of wear was characterized by the existence of a sliding distance transition. In particular, wear passed from delamination to tribo-oxidation, with a reduction in wear rate [5]. Stainless steels often display a poor tribological behaviour, which can be improved when they were hardened by incorporating N_2, TiN and Zr and forming a hardened surface zone [6]. A low temperature plasma carburising technique was developed to engineer the surfaces of austenitic stainless steels to achieve combined improvement in wear and corrosion resistance. The resultant carburised layer is free from carbide precipitates and contains a single austenite phase supersaturated

* Corresponding author. Tel.: +91 431 2503509; fax: +91 431 2500133.
E-mail address: durai@nitt.edu (M. Duraiselvam).

0925-8388/$ – see front matter © 2010 Elsevier B.V. All rights reserved.
doi:10.1016/j.jallcom.2010.06.149

Table 1
Chemical composition (wt.%) of spray powders and the counterbody.

Elements	Ni	Cr	B	Si	C	Fe	S	Mn	Mo	P
AISI 316 Substrate	14	18	–	1.0	0.08	Balance	0.03	2.00	3.00	0.045
NiCrBSiCFe Powder	Balance	13.3	3.1	3.9	0.5	3.7	–	–	–	–
EN-8 counterbody	–	–	–	0.15	0.35	Balance	–	0.6	–	0.04

with carbon. The results showed that the hard and corrosion resistant carburised layers are effective in preventing surface plastic deformation, eliminating adhesive and severe abrasive wear [7]. Tribological reactions on the friction and wear of quasicrystalline materials and coatings with two alloy compositions have been prepared by plasma and High velocity oxy fuel coating (HVOF) spraying techniques. The tribolayers were characterized by the formation of a transfer film on the counterface and densification of the coating subsurface. The wear rate appeared to be controlled by the thickness of the pore-free region formed within the coating surface zone [8]. Special attention has been paid in NiCrBSi alloys since they provide an excellent wear and corrosion resistance at high temperatures. The influence of several factors such as load, temperature, presence of reinforcement particles and the type of thermal spray technique on the wear behaviour of NiCrBSi alloy was studied by Rodriguez et al. [9]. The NiCrBSi powder was sprayed successively with plasma, flame and HVOF process. Particle characteristics obtained from different processes were compared and the quality of the formed coatings was investigated [10]. The effect of localised laser melting of plasma-sprayed NiCrBSi coatings, on the corrosion behaviour was investigated. The microstructure of the coatings was analysed by scanning electron microscope (SEM) and energy dispersive spectroscopy (EDS) analysis [11]. The effect of powder feed rate on the microstructure and mechanical properties of the supersonic plasma-sprayed NiCrBSiC coatings were investigated. The microstructure, porosity and mechanical properties of the coatings and the residual stresses at the coating surfaces were experimentally determined. Results showed that the variations of porosity, elastic moduli and microhardness of the coatings followed Weibull distribution [12]. Industrial alternative application to hard chromium plating was proposed as NiCrBSi coating. Tribological characterization was carried out in order to determine the alternative potential of NiCrBSi coatings compared to electrolytic hard chromium plating, in applications to resist wear [13]. Three groups of MoNiCrBSi coated specimens were produced with different spray distance parameter. Their microstructure and mechanical properties were analysed in order to find the optimal spray parameters that give the best structural and mechanical characteristics of the coating [14]. By employing HVOF thermal spraying, hardness and cavitation erosion resistance of steel were improved with a FeCrSiB (5.8 wt.% B) alloy coating applied to stainless steel (1Cr18Ni9Ti) substrate by HVOF thermal spraying [15]. Microstructural properties, wear resistance and potentials of thermal spraying of NiCrBSiCFe coatings for a possible replacement of hard chromium plating in mechanical parts repair was studied. A good adherence of NiCrBCSi (Fe) coating on steel substrate is explained by formation of large diffusion zone in interface after annealing and by the nature of the structure deposit duplexes [16]. NiCrBSi has been deposited onto 0Cr13Ni5Mo stainless steel using the activated combustion high velocity air fuel (AC-HVAF) technique. The structure and morphologies of the Ni-based coatings were investigated by X-ray diffraction (XRD), SEM and EDS [17]. In the above studies, the influence of temperature in the tribological properties was not emphasized. The existing studies did not focus on the operating conditions of the sliding wear and the worn tracks of the coatings were not characterized with respect to the environment. In this work, the NiCrBSiCFe was plasma sprayed on AISI 316 ASS and the tribological properties were evaluated at different temperatures such as room temperature, 150, 250 and 350 °C using a pin-on-disc tribometer. The influence of microstructure and hardness on the wear resistance was explained using SEM micrographs and mechanical properties of the coating. The wear mechanism was identified by correlating SEM and XRD analysis.

2. Experimental procedure

2.1. Materials and plasma spraying process

The as-received AISI 316 ASS sheets were machined into a disc of 100 mm diameter and 4 mm thickness. It was degreased with acetone and grit blasted to a R_a value of 10 μm to improve the surface roughness. Commercially available pure Micro-Melt® B-60 NiCrBSiCFe alloy powder was used as a raw material. The powder was supplied by Carpenter Powder Products Inc., U.S.A. The morphology of NiCrBSiCFe powder particles was analysed by SEM. An EN-8 medium carbon steel pin was used as a counterface material. The chemical composition of substrate, powder and counterbody is shown in Table 1. During plasma spraying, the spray gun (Sulzer Metco SST-24) was stationary and the specimen was mounted on a rotating table. The coating feedstock material was injected vertically into the plasma jet by argon (Ar) carrier gas for primary flow and hydrogen gas (H_2) for secondary flow. The plasma coating was performed up to 500 μm thickness. The selected spray parameters are given in Table 2.

2.2. Wear test

Wear tests were carried out under dry sliding condition on a DUCOM pin-on-disc tribometer, model TR-20-M-106 as shown in Fig. 1. The linear variable differential transducer (LVDT) probe was positioned on the weights to measure displacement and the load cell to sense the tangential force. ASTM G99-05 [18], the standard test method for wear testing with a pin-on-disc apparatus was slightly deviated by having plasma-sprayed steel disc as a specimen for characterizing the coating. The counterface material, EN-8 medium carbon steel, was prepared in the form of pin with a dimension of 31 mm height and 6 mm diameter. The pin was made to slide on the coated steel disc at 1.0 m/s sliding speed under the load 20 N for 2000 m sliding distance. The NiCrBSiCFe plasma coated samples were polished by surface grinding to attain the surface roughness value $R_a \sim 1$ μm. The wear tests were conducted at temperatures such as room temperature (35), 150, 250 and 350 °C. Before and after test, the plasma-sprayed disc substrates were ultrasonically cleaned, dried and weighed using an electronic analytical balance to an accuracy of 0.1 mg. By using the data acquisition system, the depth of wear and the frictional force were recorded automatically with respect to time. Using the mass loss, the volume loss was computed using Eq. (1). The wear resistance was calculated using Eq. (4). The measured frictional force from the data acquisition system was used to compute coefficient of friction (CoF) using Eq. (5).

$$\text{volume loss}\,(\text{mm}^3) = \left(\frac{\text{mass loss}}{\rho}\right) \times 1000 \quad (1)$$

Table 2
Selected processing parameters.

Spray parameter	Value
Substrate	AISI 316 ASS
D.C. current (A)	480
D.C. volts (V)	70
Primary gas flow rate (SLPM) Argon	150
Hydrogen	15
Feedstock carrier gas flow rate (SLPM) Argon	37
Powder flow rate (g/min)	120
Standoff spray distance (mm)	125
Scanning velocity (mm/s)	6
Coating thickness (μm)	500

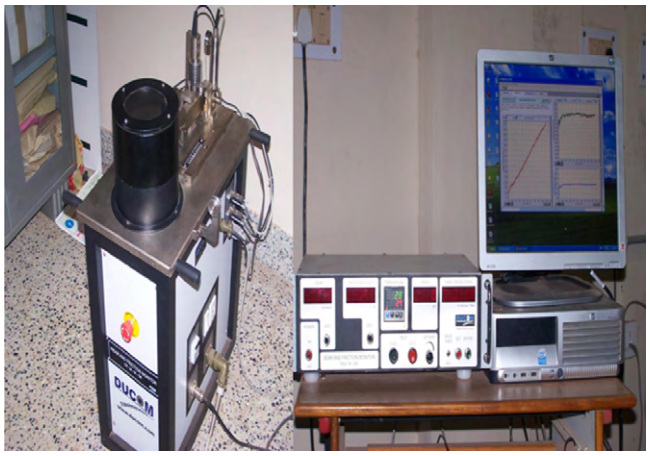

Fig. 1. Schematic setup of wear test.

$$\text{coating density}\,(\rho) = \rho_1 \left(\frac{m_a}{m_a - m_1}\right) \quad (2)$$

where ρ_1 is the density of water 1 g/cm^3 at room temperature, m_a the weight of the plasma coating in air (g) and m_1 is the weight of plasma coating in water (g).The wear rate and wear resistance was calculated by the following equations:

$$\text{wear}\left(\text{mm}^3/\text{m}\right) = \frac{\text{volume loss}}{\text{sliding distance}} \quad (3)$$

$$\text{wear resistance}\left(\text{m}/\text{mm}^3\right) = \frac{\text{sliding distance}}{\text{volume loss}} \quad (4)$$

$$\text{coefficient of friction}, \mu = \frac{F}{N} \quad (5)$$

where F is the frictional force in N, N is normal applied load in N.

2.3. Coating characterization

The following methods were used to characterize the coatings.

2.3.1. Microstructural and XRD characterization

The plasma-sprayed AISI 316 ASS samples were sectioned, polished and etched with Nital. The etched specimens were studied by optical microscopy (OM). The micrograph of EN-8 medium carbon steel was also analysed. The worn tracks of the plasma-sprayed specimens were analysed using SEM (HITACHI S 3000H) to identify the mode of material loss during sliding at different temperatures. The worn debris of the uncoated AISI 316 ASS and NiCrBSiCFe coated discs at room temperature were carefully collected separately after the completion of the experiments. The morphology of the wear asperities collected was characterized by SEM. The phase constitution of uncoated, as-sprayed and worn out specimens was evaluated by XRD analysis with CuKα radiation source (D/MAX ULTIMA III, Rigaku Corporation, Japan) operating at 30 mA and 40 kV. The set scanning speed and the scanning range are 2°/min and 10–80°, respectively. A sample of as-sprayed plasma coated surface was first cut suitably and analysed by SEM.

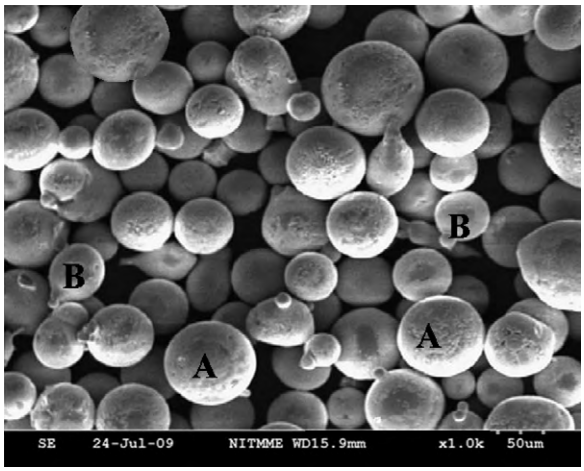

Fig. 2. SEM morphology of NiCrBSiCFe powder: (A, spherical powder; B, the spherical powder with satellite formation).

2.3.2. Microhardness and density measurement

The microhardness was measured using Zwick MHT Vickers hardness tester at a load of 300 g for 20 s. According to the weight fraction and density of each element in NiCrBSiCFe the theoretical density was calculated as 8.146 g/cm^3 [19]. In order to determine the actual density, the NiCrBSiCFe coating was mechanically peeled off from the substrate and measured using Archimedes principle as per Eq. (2). The average actual density of the coating was 8.116 g/cm^3.

3. Results and discussions

3.1. Powder characterization

The morphology of NiCrBSiCFe powder particles was investigated using SEM, which is shown in Fig. 2. The powder consists of gas atomized spherically shaped particle. Small strings like pro-

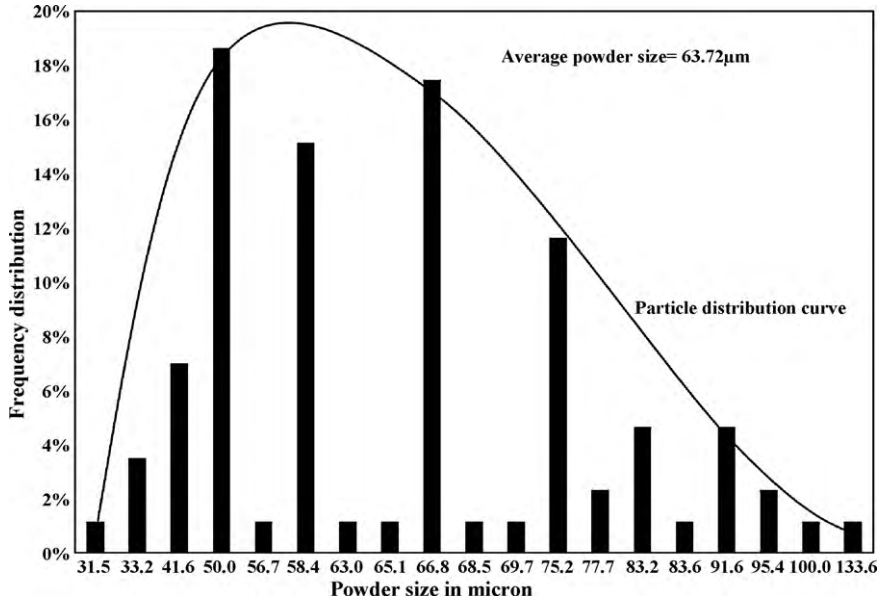

Fig. 3. Particle size distribution of the NiCrBSiCFe powder.

trusions named satellite formation were visible with a size of 3–4 μm are shown. This was actually a minor defect in gas atomized powder manufacturing process, which was rarely noticed. The particle size was calculated and the frequency of the particle size was measured, which is shown in Fig. 3. The mean particle size of the feedstock powder used in the present study was identified as 63.72 μm. The particle distribution curve in the graph depicted the frequent occurrences of powders of sizes ranging 50–66 μm [15]. The nature of the powder microstructure revealed the size and shape distribution of the powder. It was further inferred that plasma spraying of the powder was possible without any drastic microstructural evolution. The rough state preparation of the powder NiCrBSiCFe by the atomization process, gives an aspect called refractory property that allows it to withstand relatively high temperatures [16].

3.2. Coating microstructure

The cross-sectional images of the microstructure of NiCrBSiCFe coatings are shown in Fig. 4(a) and (b). The improved roughness by grit blasting was explicitly visible as undulations on the interface region aided for a good metallurgical boding. The micrograph indicated that the physical bonding between the coating and the interface was intact. Absence of pores in the interface region substantiated that the bonding was intact. The microstructure of the coatings showed elongated splats of molten powder forming a lamellar structure. This structure was responsible for the higher hardness, which offered superior wear resistance. The absence of microcracks showed that the processing parameters selected in this study have ensured a good quality of plasma-sprayed coatings. The microstructure of the counterbody, EN-8 medium carbon steel pin is shown in Fig. 4(c). They were classed as a hard ferro-magnetic group. The presence of frequent carbides in the microstructure was responsible for the higher hardness.

3.3. Microhardness characterization

The Vickers hardness of AISI 316 ASS substrate and EN-8 medium carbon steel pin was 223 and 302 $HV_{0.3}$, respectively. Three distinct regions were distinguished in the hardness profile namely plasma-sprayed coating, interface and substrate. The microhardness of the cross section of the NiCrBSiCFe coatings as a function of distance from the coating substrate is shown in Fig. 5. The microhardness of the NiCrBSiCFe plasma coating is found to vary with the distance from the coating-substrate interface. Coating microhardness values were found to be in the range of 730–918 $HV_{0.3}$. The maximum value of about 918 $HV_{0.3}$ was obtained in the top of the coating, which may be the point of the boride formed during plasma spraying. The average microhardness value is 822 $HV_{0.3}$.The interface region showed an intermediate hardness values ranging 294–398 $HV_{0.3}$. The increase of hardness of AISI 316 ASS substrates due to the plasma-sprayed coating was responsible for the superior wear resistance (540 m/mm^3).

3.4. Friction and wear behaviour

The consolidated wear with respect to time at different temperatures is shown in Fig. 6. The wear was primarily dominated by plastic deformation. In uncoated AISI 316 ASS substrate, it was inferred that the wear at 250 °C was higher than that of the rest of the temperatures. The wear rate at 350 °C was initially found to be higher, but as time proceeds, the oxide layer formations considerably reduced the wear. The hard oxide layers formed might have induced slipping in sliding wear. Except in 350 °C, the uncoated

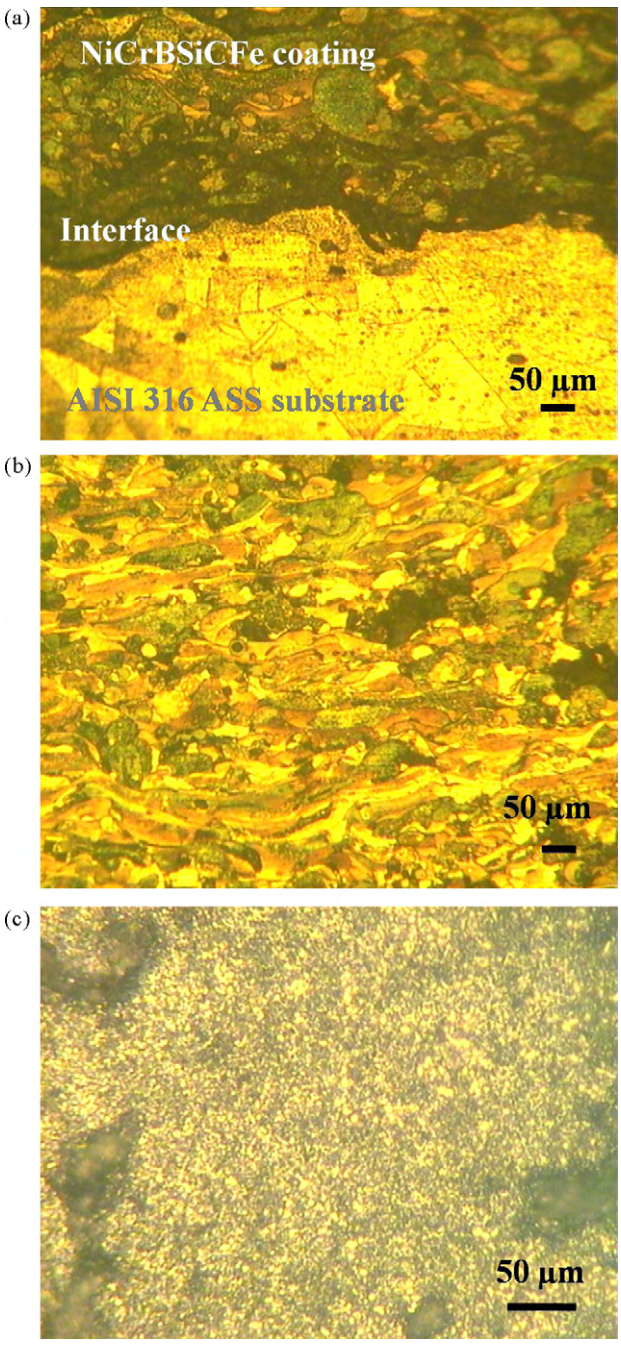

Fig. 4. Cross-sectional micrographs: (a) interface and coating, (b) lamellar structure of the as-sprayed structure of the NiCrBSiCFe plasma-sprayed coating, (c) EN-8 medium carbon steel counterbody.

AISI 316 ASS showed severe wear in all operating temperatures. In contrast, the NiCrBSiCFe coated samples showed very less wear in all temperatures. Relative sliding between the contacting surfaces leads to the rupture of these junctions and subsequent material transfer from one surface to the other, in addition to the production of debris and material loss. The presence of a lubricating oxide film reduces the tendency for adhesive wear occurrence [21]. Notably in 350 °C, the wear rate was marginally lesser than the rest of the temperatures due to the initiation of oxide layers, which was also substantiated by XRD analysis (Fig. 7.) The CoF for the uncoated AISI 316 ASS varies between 0.2 and 0.7 in all the temperatures. In NiCrBSiCFe coated discs, the CoF was found to be relatively lesser and was ranging from 0.1 to 0.5 in all temperatures. In

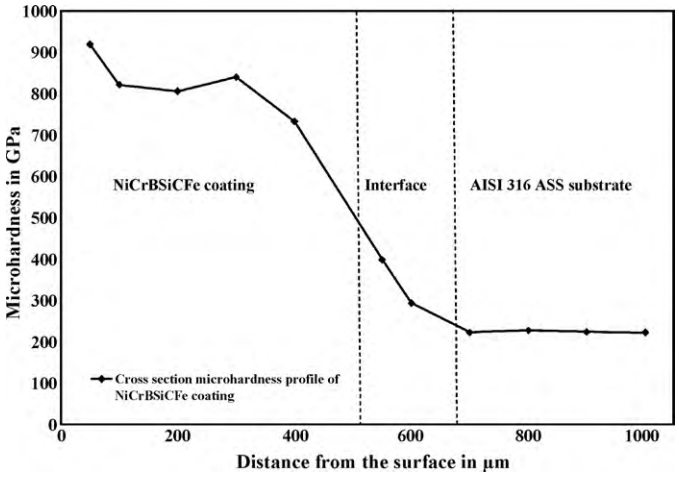

Fig. 5. Microhardness variation of the NiCrBSiCFe coatings as a function of the distance from the surface.

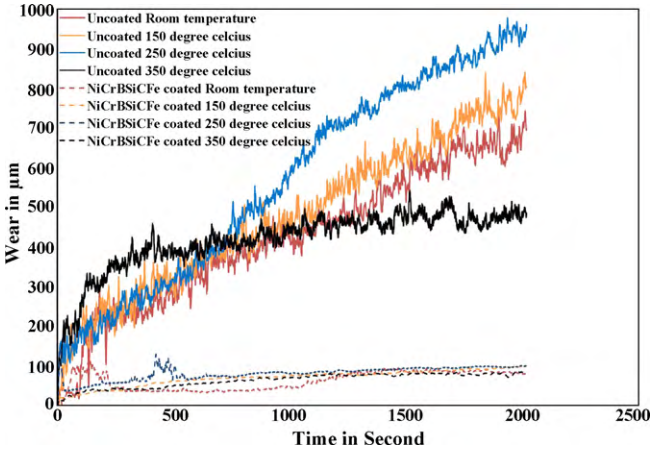

Fig. 6. Variation of wear with respect to time and temperature.

coated samples worn at 350 °C, the COF was in the lower optimum range of 0.1–0.2. This optimum value might be due to the oxide formations like Fe_3O_4 and CrO_3 in the interface at 350 °C. The oxide formations were explained in detail in Section 3.5. The wear resistances of the uncoated and plasma-sprayed steel substrates are shown in Fig. 8. The highest wear resistance of 9.62 m/mm^3

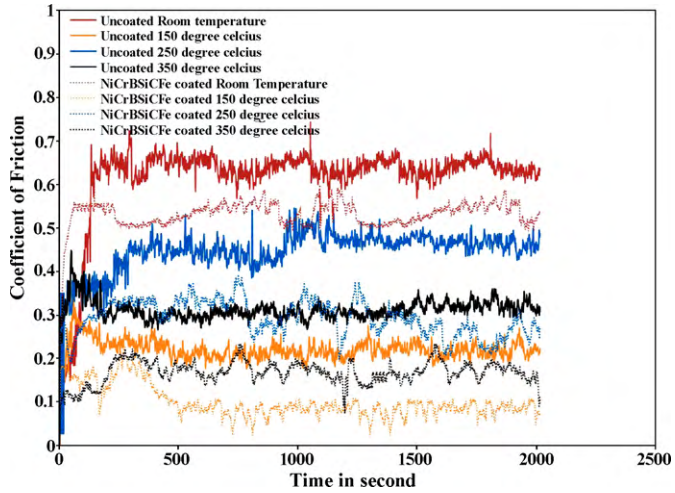

Fig. 7. Variation of coefficient of friction with respect to time and temperature.

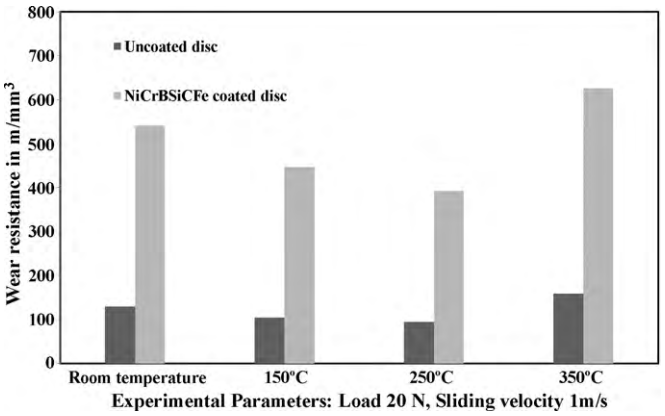

Fig. 8. Comparison of wear resistances of uncoated and NiCrBSiCFe coated samples with respect to temperature.

was recorded for the plasma-sprayed steel substrate at 350 °C.

3.5. Phase identification by XRD

The consolidated XRD patterns of the uncoated AISI 316 ASS substrates were shown in Fig. 9. It reveals the peaks having the phases of γ-Iron (fcc) in all operating temperatures. In addition, at 350 °C the XRD showed the CrO_3 phase. The XRD patterns of the as-sprayed NiCrBSiCFe plasma coated surface and the worn tracks of the plasma coated substrates are shown in Fig. 10. The peaks reveal the presence of certain intermetallics namely Fe_3B [17], $Cr_{1.12}Ni_{2.88}$ and Ni_3B [11]. It is also clear that there are no new phases formed in the coating during the thermal spray process. The major intermetallic found in the coated surface was $Cr_{1.12}Ni_{2.88}$ in all operating temperatures. In worn track at 350 °C, the presence of Fe_3O_4 and CrO_3 was evident. The presence of these oxide phases justified the lesser wear at 350 °C.

3.6. Worn surface and debris characterization by SEM

The as-sprayed NiCrBSiCFe plasma coated surface is shown in Fig. 11(a). The coated surface when analysed by SEM revealed the presence of small voids. The as-sprayed surface also showed the sparsely distributed unmelted spherical particles. These unmelted

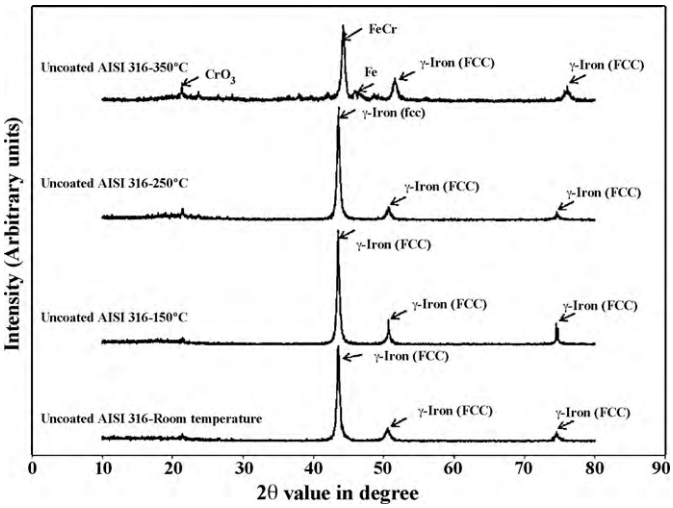

Fig. 9. XRD pattern showing phases in worn track of uncoated AISI 316 ASS substrates.

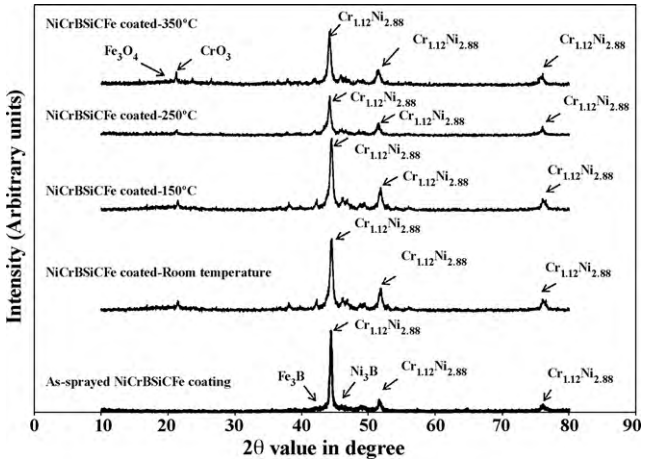

Fig. 10. XRD pattern showing phases in the as-sprayed NiCrBSiCFe coating and worn tracks of the coated samples at various temperatures.

spherical powder particles were visible due to the high flight in velocity of the particle. The surface morphology of NiCrBSiCFe coated specimen worn at room temperature is shown in Fig. 11(b). The worn track exhibited delaminated layer with small amount of scabs and debris. As the time progresses, the delaminated layer may peel off and lead to considerable material loss.

The wear track formed by sliding wear had a very smooth and shiny appearance. The worn surface morphology of the NiCrBSiCFe coated sample at 150 °C is shown in Fig. 11(c). The mode of wear was found to be exfoliation. Normally exfoliation mode is comparatively severe than delaminated type of material removal. Exfoliation of thick flakes was generally aided by crack formation. The consequence of this mode of material removal was sub surface cracking which in turn leads to the removal of subsequent layers. The wear resistance of this operating temperature 150 °C was found to be lesser than that of the room temperature. The mode of material removal at 250 °C was ploughing. These ploughing marks normally start with the score lines parallel to the sliding direction and later on these lines capitalize to form plough markings. The advanced stage

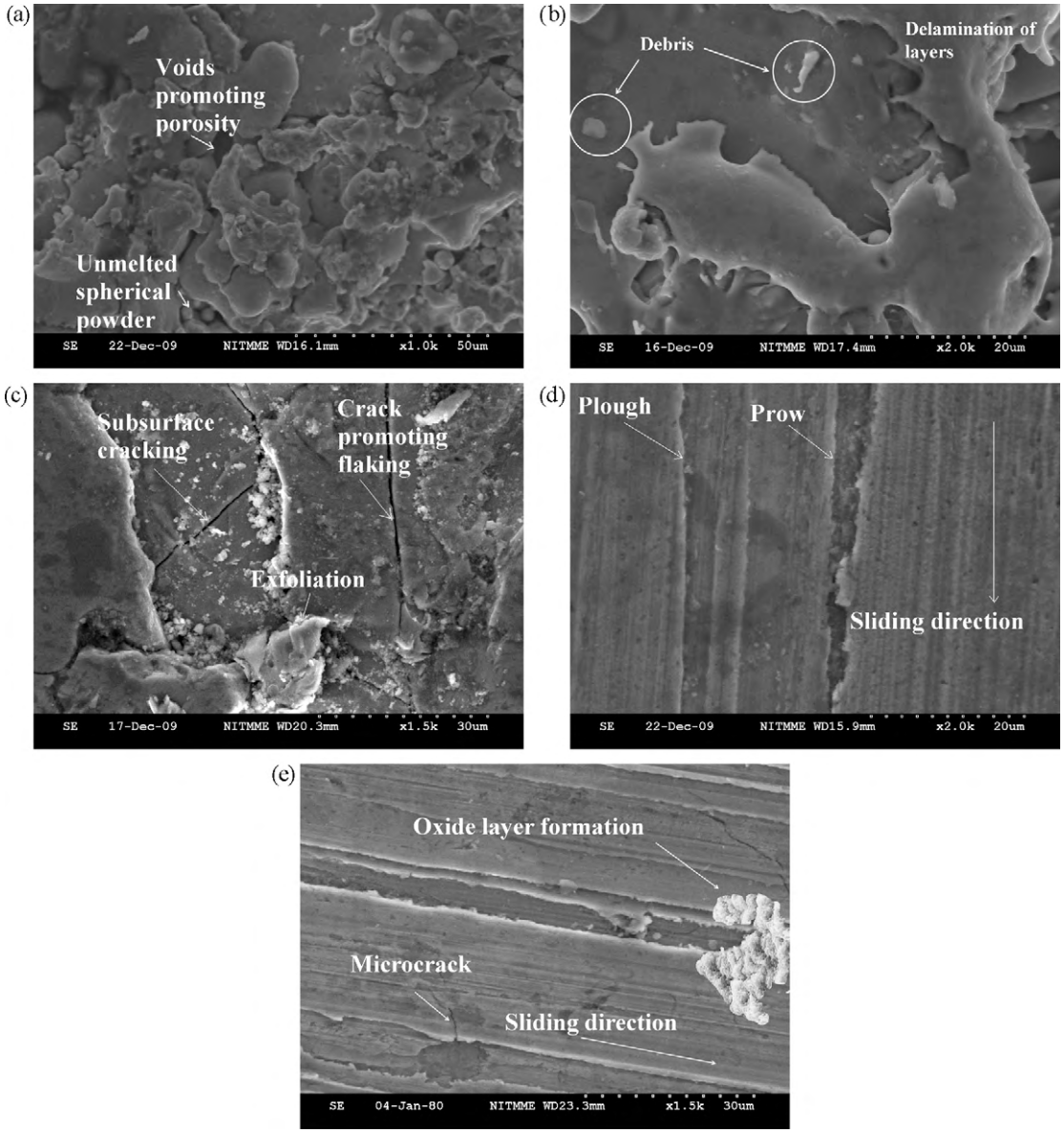

Fig. 11. SEM picture of the NiCrBSiCFe coated surfaces: (a) as-sprayed NiCrBSiCFe plasma coated surface, (b) worn surface at room temperature (c) worn surface at 150 °C (d) worn surface at 250 °C (e) worn surface at 350 °C.

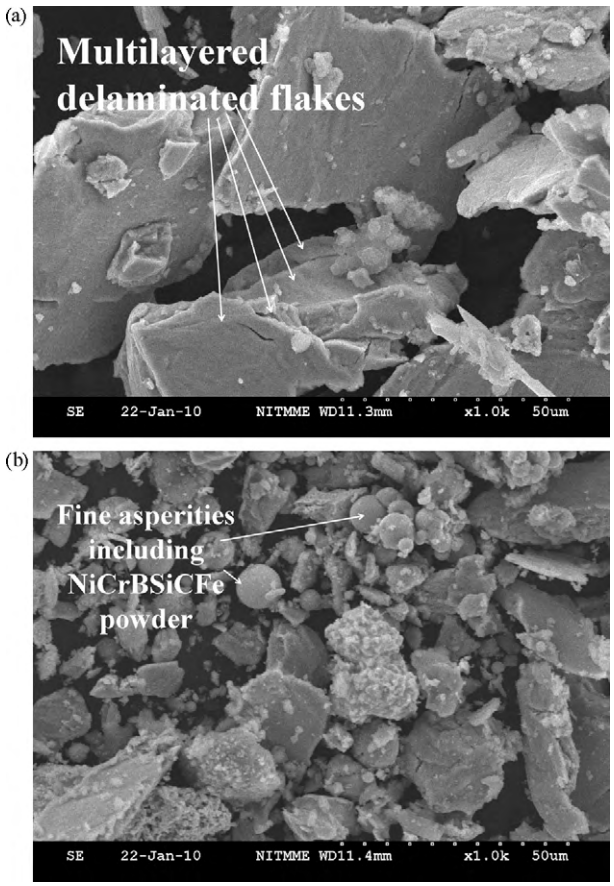

Fig. 12. SEM picture of the asperities: (a) uncoated AISI 316 ASS debris, (b) NiCrBSiCFe coated debris showing powder inclusion.

in plough mode of material removal is prow formations. The prow formations were the end result of frequent ploughings on the same instance. This mode leads to more material loss which is evident from Fig. 11(d). Dry sliding leads to high local pressure between contacting asperities, which results in plastic deformation, adhesion and the consequent formation of junctions locally. The worn surface morphology of NiCrBSiCFe coated sample at 350 °C is shown in Fig. 11(e). The mode of material removal is shallow ploughing. The score lines, which run always parallel to the sliding direction, were explicitly seen. As a result of the interface temperature induced at asperity contacts during sliding, an oxide film was produced,

this surface oxide protects the underlying surface by reducing wear rate [20]. The interesting phenomenon happened in the interface of the counterbody and the coated substrate is oxide formation. The oxide formation is visible in SEM. These oxide layers could be of Fe_3O_4 and CrO_3, which was confirmed by XRD analysis (Fig. 10). Oxide films formed during the contact play a protective part, eliminating the chances of excessive material loss. This property of the oxide reduced the severity of wear [21].

Dry sliding wear leads to the removal of material from the surface by the formation of chips, shavings and fragments called debris. The geometry of the worn surface and a groove formed depends on the size and shape of the worn debris (abrasive particle) [21]. At room temperature, the worn debris of the uncoated AISI 316 ASS substrate and NiCrBSiCFe coated discs were collected after the completion of the experiment. The debris with asperities of the uncoated AISI 316 ASS substrate is shown in Fig. 12(a). The asperities were characterized by flakes showing multilayered structure. The distinct flake formations justified the mode of material loss by plastic deformation. The entrapment of the debris and asperities between the sliding contact surfaces would obviously increase wear rate of AISI316 ASS substrates by the mechanisms of three-body abrasion (rolling), where the entrapped particles serve as an abrasive [11]. The worn debris of the NiCrBSiCFe coated substrate is shown in Fig. 12(b). The debris was finer in size when compared to the uncoated AISI 316 ASS debris. The presence of unmelted spherical powders peeled off from the coating was sparsely and distinctly visible from the observation. The geometry of the asperities showed lesser severity in enhancing further wear to the sliding process, leading to the superior wear resistance of the NiCrBSiCFe plasma-sprayed AISI 316 ASS substrates.

4. Conclusions

From the experiments conducted on uncoated and NiCrBSiCFe plasma-sprayed AISI 316 ASS substrates at various operating temperatures, the following conclusions can be drawn.

- The NiCrBSiCFe was plasma sprayed on AISI 316 ASS to a thickness of up to 500 μm. The coatings produced were metallurgically bonded to the substrate and free from any defects.
- The improvement in hardness up to an average value of 822 $HV_{0.3}$ of AISI 316 ASS from 223 $HV_{0.3}$ was achieved by NiCrBSiCFe plasma spraying primarily contributed to the improvement of wear resistance.
- The plasma-sprayed NiCrBSiCFe coating exhibited up to four times increase in wear resistance compared to the uncoated AISI 316 ASS substrates.
- The superior wear resistance of the NiCrBSiCFe coated samples in the operating temperature 350 °C justifies the applicability of the coating for high temperature applications involving sliding contact.
- At 350 °C, the formation of oxide layers such as Fe_3O_4 and CrO_3, confirmed by XRD analysis further reduced the severity of wear. These protective oxide layers formations acted as a lubricant between sliding surfaces which reduced the severity of material loss.
- The worn surface morphology analysed by SEM revealed the presence of shallow ploughing at 350 °C. This was a minimal material removing mode which excluded the chance of more material loss.
- The geometry of the worn asperities of the NiCrBSiCFe plasma spayed coating was finer compared to the uncoated specimens. This property reduced the intensity of wear rate in coated specimens. The SEM results were found to be in accordance with the sliding wear test results.

References

[1] A.F. Smith, Wear 19 (1986) 3–10.
[2] A.F. Smith, Tribol. Int. (1986) 10003–10008 (0301-679X).
[3] H. Hemmes, P. Splittgerber-Hünnekes, W. Aschern, T. Kachlicki, M. Smithers, H. Rogalla, D. Stöver, J. Alloys Compd. 195 (1993) 283–286.
[4] L.C. Betancourt-Dougherty, R.W. Smith, Wear 217 (1998) 147–154.
[5] G. Straffelini, D. Trabucco, A. Molinari, Metall. Mater. Trans. A 33A (2002) 613–624.
[6] H. Dogan, F. Findik, O. Morgul, Mater. Des. 23 (2002) 605–610.
[7] Y. Sun, T. Bell, Wear 253 (2002) 689–693.
[8] E. Fleury, Y.C. Kim, J.S. Kim, D.H. Kim, W.T. Kim, H.S. Ahn, S.M. Lee, J. Alloys Compd. 342 (2002) 321–325.
[9] J. Rodriguez, A. Martin, R. Fernandez, J.E. Fernandez, Wear 255 (2003) 950–955.
[10] M.P. Planche, H. Liao, B. Normand, C. Coddet, Surf. Coat. Technol. 200 (2005) 2465–2473.
[11] C. Navas, R. Vijande, J.M. Cuetos, M.R. Fernández, J. de Damborene, Surf. Coat. Technol. 201 (2006) 776–785.
[12] X.C. Zhang, B.S. Xu, Y.X. Wu, F.Z. Xuan, S.T. Tu, Appl. Surf. Sci. 254 (2008) 3879–3889.
[13] N. Serres, F. Hlawka, S. Costil, C. Langlade, F. Machi, A. Cornet, Surf. Coat. Technol. 204 (2009) 197–204.
[14] M. Mrdak, A. Vencl, M. Cosic, FME Trans. 37 (2009) 27–32.
[15] Y. Wu, P. Lin, Z. Wang, G. Li, J. Alloys Compd. 481 (2009) 719–724.

[16] S. Abdi, S. Lebaili, Phys. Proc. 2 (2009) 1005–1014.
[17] S. Liu, X. Zheng, G. Geng, Mater. Des. 31 (2010) 913–917.
[18] ASTM G99-95, ASTM G99-95a (reapproved 2000): standard test method for wear testing with a pin on disk apparatus, 1995.
[19] Y.Y. Wang, C.J. Li, A. Ohmori, Surf. Coat. Technol. 200 (2006) 2923–2928.
[20] R. Gonzĭalez, M.A. Garcia, I. Penuelas, M. Cadenas, Ma. del Rocio Fernandez, A. Hernandez Battez, D. Felgueroso, Wear 263 (2007) 619–624.
[21] I.M. Hutchings, Tribology, Friction and Wear of Engineering Materials, Butterwort-Heinemann, 1992.